

# Preliminary Analysis of Spherical Iron-rich Particles Extracted from Moto-Ujina Beach Sand as a Possible Tracer for the Hiroshima Black Rain

Satoru Endo<sup>a,\*</sup>, Tsuyoshi Kajimoto<sup>a</sup>, Kenichi Tanaka<sup>b</sup>, Hiroki Higuchi<sup>a</sup>, Satoshi Fukutani<sup>c</sup>, Koichi Takamiya<sup>c</sup>, Makoto Maeda<sup>d</sup>, Yasuhito Igarashi<sup>c</sup>

<sup>a</sup>Quantum Energy Applications, Graduate School of Advanced Science and Engineering, Hiroshima University, 1-4-1 Kagamiyama, Higashi-Hiroshima, Hiroshima 739-8527, Japan

<sup>b</sup>Department of Physics, Kyoto Pharmaceutical University, 5 Misasaginakauchi-cho, Yamashina-ku, Kyoto 607-8414, Japan

<sup>c</sup>Institute for Integrated Radiation and Nuclear Science, Kyoto University, 2 Asashiro-Nishi, Kumatori-cho, Sennan-gun, Osaka 590-0494, Japan

<sup>d</sup>Natural Science Center for Basic Research and Development (N-BARD), Hiroshima University, 1-3-1 Kagamiyama, Higashi-Hiroshima, Hiroshima 739-8526, Japan

Received December 10, 2022; Accepted February 6, 2023; Published online February 15, 2023

Sand samples were collected from Moto-Ujina Beach, Hiroshima in order to analyze spherical iron-rich particles, which may have been produced by the Hiroshima atomic bomb explosion. Spherical iron-rich particles (5.86 g) were extracted from the beach sand by magnetic collection. The extracted particles were analyzed by scanning electron microscopy-energy dispersive X-ray spectrometry (SEM-EDS) and  $\gamma$ -ray spectroscopy using a Ge detector. The SEM-EDS analysis revealed that the spherical particles were composed mainly of Si and O, and contained Na, Mg, Al, P, K, Ca, Ti, V, and Fe. The Ge detector detected 662 keV  $\gamma$ -rays with a count rate of  $2.6 \times 10^{-4}$  cps and the radioactivity of  $^{137}\text{Cs}$  was calculated to be  $1.3 \pm 0.5$  mBq g<sup>-1</sup>. Although we could not definitively conclude that the particles originated from the atomic bomb explosion, we could not rule out the possibility that some of these iron oxide particles were formed by vaporization and condensation of bomb material and dust that agglomerated during the Hiroshima bomb explosion.

## 1. Introduction

In summer 2021, policy decisions were made to provide relief to victims thought to be affected by the “black rain” caused by the atomic bomb explosion. However, even though more than three quarters of a century has passed since the atomic bombs were detonated, little is understood about the fundamental and material sciences of the black rain. In this study, we search for traces of the black rain by using new methods developed for research into the Fukushima Daiichi Nuclear Power Plant (FDNPP) accident. Despite numerous attempts, including the 1976 and 1979 Ministry of Health and Welfare-led studies, black rain regions have never been identified by measuring only the radionuclides that remain in the soil (e.g., Hiroshima City 2011, 2013)<sup>1,2</sup>. This is because the radionuclide signature from the atomic bomb explosion was drowned out by the superposition of radionuclides from the global fallout caused by atmospheric nuclear experiments in the 1960s and 1970s. Therefore, we need to find new tracers for the black rain.

Wannier et al.<sup>3</sup> reported that unique types of melt debris of high-temperature origin (>1800 °C) are contained in the sand at Moto-Ujina Beach, Hiroshima, Japan. They isolated a group of particles consisting of spherical silica and iron oxide particles, deformed candy-like glass particles containing air bubbles, and many particles that also contained air bubbles and that were melted and glazed after they were crushed. These particles are coarse (hundreds of micrometers in size) and abundant about ten thousand particles in total). Wannier et al.<sup>3</sup> estimated the abundance of the particles to be about

3000 tons around the coast of Hiroshima, and thus they concluded that on balance, the evidence suggested that the origin of the particles was linked to the nuclear explosion of August 6th, 1945. Similar spherical particles were also identified following the FDNPP accident<sup>4-8</sup> in 2011, although the size range was far smaller. Therefore, we could take a similar approach to identifying black rain particles as was applied to the Fukushima particles. Accordingly, we have added the collection and analysis of spherical particle samples from the Moto-Ujina Beach to the objectives of our reinvestigation of the black rain.

In this paper, we report an overview of sand sampling from Moto-Ujina Beach and the method of spherical particle extraction, and we present the results of the scanning electron microscopy-energy dispersive X-ray spectrometry (SEM-EDS) analysis and  $\gamma$ -ray spectrometric measurements with a Ge detector for the extracted particles.

## 2. Materials and methods

**2.1 Sampling.** The sampling was conducted on April 26 and August 26, 2021. Five lots of sand samples were collected at each of the sampling locations (Uj01 to Uj05) on Moto-Ujina Beach, Hiroshima City, at intervals of several meters (Fig. 1). The sand samples were separately collected at depths of 0–5 cm and 5–10 cm from the surface using a garden shovel. The amounts of each sand sample are listed in Table 1.

As explained below, particles originating from the atomic bomb are expected to be iron-rich because the major constituent of the atomic bomb dropped over Hiroshima was made of steel. In particular, the molten particles are believed to be

\*Corresponding author. E-mail: endos@hiroshima-u.ac.jp

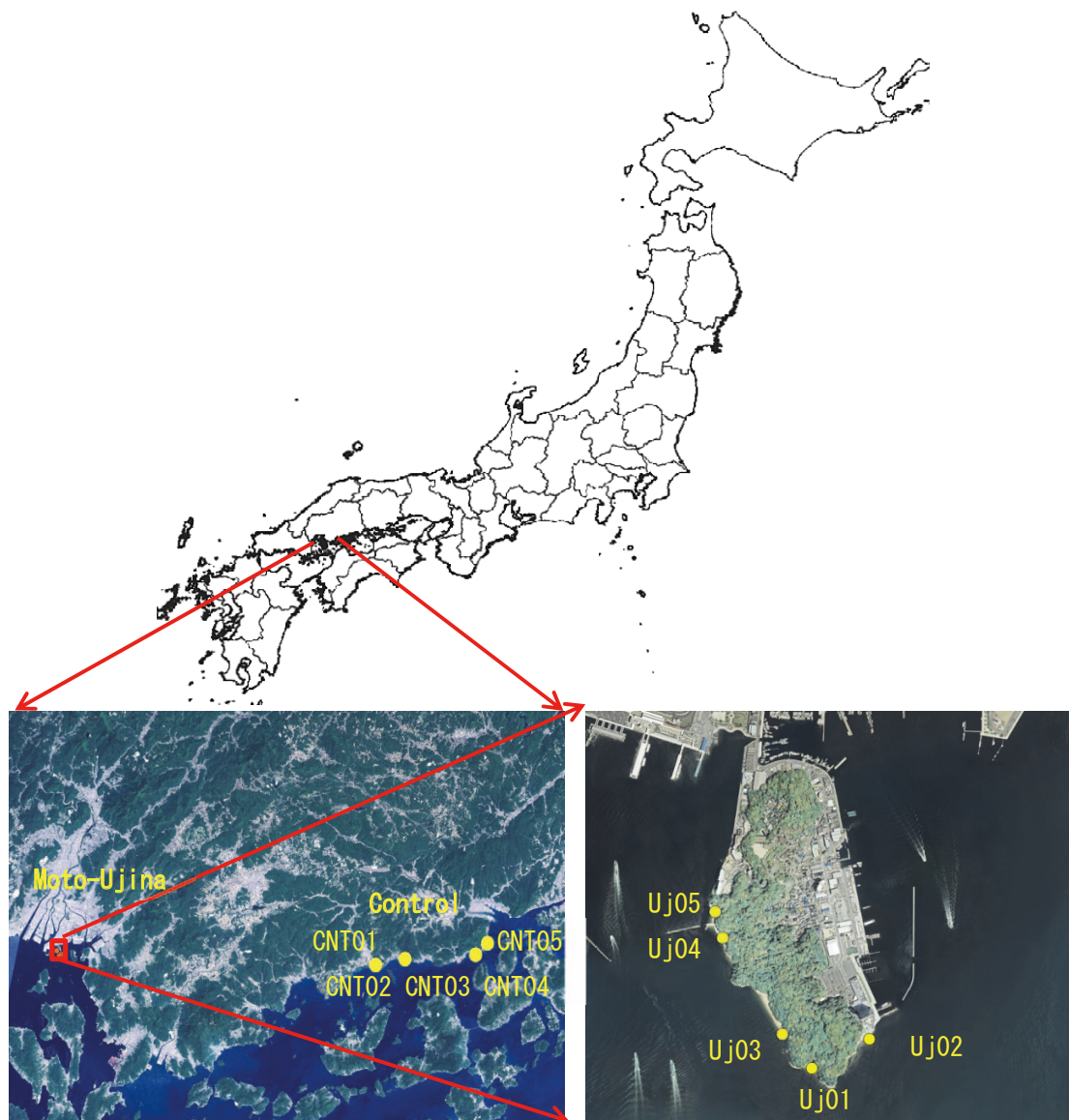


**Figure 1.** Sampling locations shown with an electronic map using GSI XYZ tiles (GSI 2021).

**TABLE 1: GPS addresses of sampling locations.**

Sampling location	Location	Longitude	Latitude	Number of points
Uj01	Moto-Ujina Beach	132.4621	34.3407	5
Uj02	Moto-Ujina Beach	132.4645	34.34168	5
Uj03	Moto-Ujina Beach	132.4609	34.34186	5
Uj04	Moto-Ujina Beach	132.4583	34.34517	5
Uj05	Moto-Ujina Beach	132.458	34.34605	5
CNT01	Matoba Beach, Takehara	132.9214	34.32575	1
CNT02	Matoba Beach, Takehara	132.9226	34.32567	1
CNT03	Tadanomi-Nagahama, Takehara	132.967	34.33592	1
CNT04	Saizaki-Kuwaki, Mihara	133.0689	34.34342	1
CNT05	Sunami Seaside Park, Mihara	133.0823	34.35358	1

iron-rich because the steel base material is thought to have melted and agglomerated in the fireball of the atomic bomb. During sampling, iron-rich materials (about 61 g) were collected from the sandy beach at Uj01 using a magnetic toolbar (GISUKE) measuring  $1.5 \times 20$  cm.

Sand samples were also collected as control samples on June 1, 2021 from in Takehara and Mihara, 40–50 km from

Moto-Ujina Beach, which have sandy beaches similar to Moto-Ujina Beach. The five sampling locations at Moto-Ujina Beach as well as the locations of the control samples are shown in Fig. 1 on the electronic topographic map (tile), Geospatial Information Authority of Japan (GSI) <sup>9</sup>, and the details are also listed in Table 1.

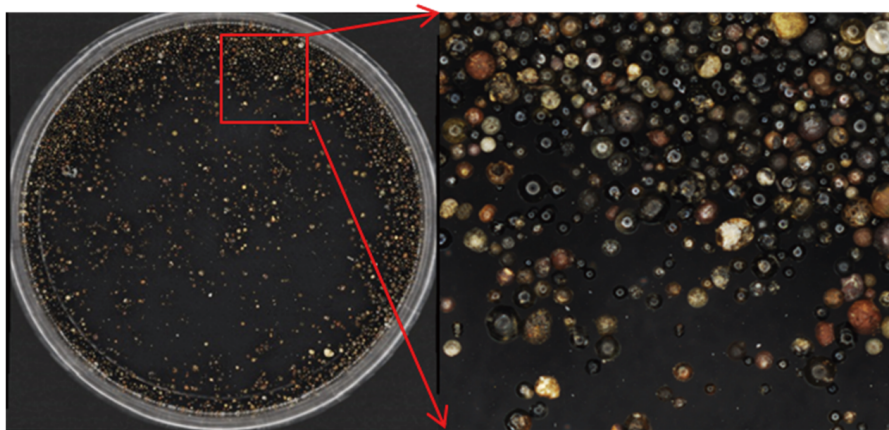


Figure 2. Photograph showing an example of the extracted particles from a Moto-Ujina Beach sand sample.

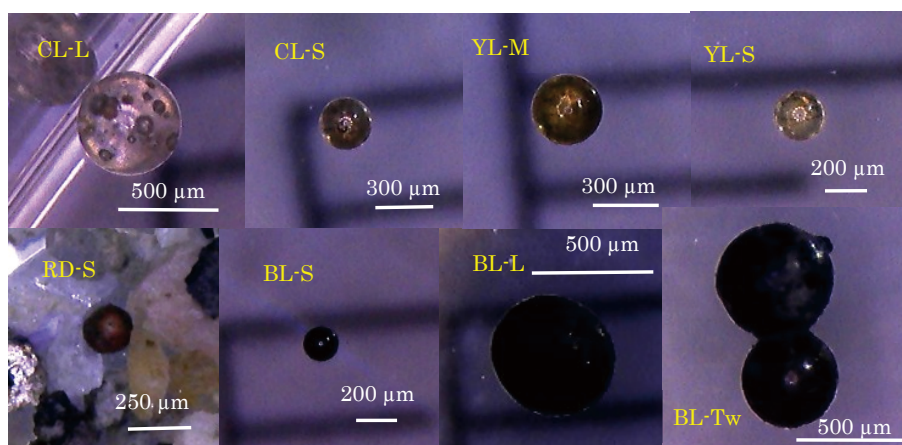


Figure 3. Photograph of spherical particles used for SEM-EDS analysis.

**2.2 Sample preparation.** To remove sea salt from the sand, the sand samples were immersed in tap water that was three times the volume of the sand sample and left to stand for several minutes, and then the water was discarded. This process was repeated five times. Then, a small amount of ethanol was added to the washed and water removed samples, which were dried under a stream of warm air for several hours. After washing, the samples were sieved with a 1 mm mesh to remove large sand grains and shells.

**2.3 Extraction of spherical particles.** If the particles originated from the atomic bomb explosion, they would contain iron from the vaporized bomb material, and thus a magnet was used to extract the particles. The top of the thinly spread sand was scanned with a magnet tool, and the grains sticking to the magnet were extracted. Spherical particles were picked out from the extracted grains. A photograph of the extracted particles from sample Uj05-02U is shown in Fig. 2. The particle size of the dispensing extracted particles (0.14 g, 4805 particles) was measured with a digital microscope (HRX-01, Hirox Co., Ltd.).

**2.4 SEM-EDS measurements.** From the extracted spherical particles, four types of particles of different colors and sizes (transparent: CL; yellowish transparent: YL; black: BL; red: RD, small: S; medium: M; large: L; twin: Tw) were selected for SEM-EDS analyses with a scanning electron microscope (S-5200, Hitachi High-Technologies Corp.) and an X-ray spectrometer (Genesis XM2, EDAX). Photographs of the spherical particles used for SEM-EDS analyses are shown

in Fig. 3.

**2.5 Ge measurement.** A total of 5.86 g of spherical particles comprising 3.69 g extracted from the 50 sand samples and 2.17 g extracted from the 61 g of iron-rich materials collected using the magnetic tool bar was wrapped in pharmaceutical wrapping paper and vacuum-packed with a food vacuum sealing system (Shinku-Pakken, Kurashi-no-Koubin) into a flat plate of  $3 \times 4$  cm for  $\gamma$ -ray spectroscopy with a Ge semiconductor detector (GMX-30200-P, Ortec). The Ge measurement were carried out for 700,000 s on day 8 after packing. The measurement efficiency of the Ge detector was determined using a planar standard source (MX421, Japan Isotope Association), which is a 50-mm-diameter planar radiation source consisting of nine radionuclides ( $^{51}\text{Cr}$ ,  $^{54}\text{Mn}$ ,  $^{57}\text{Co}$ ,  $^{60}\text{Co}$ ,  $^{85}\text{Sr}$ ,  $^{88}\text{Y}$ ,  $^{109}\text{Cd}$ ,  $^{137}\text{Cs}$ , and  $^{139}\text{Ce}$ ) encapsulated in a 4-mm-thick acrylic disk with a diameter of 60 mm. The PHITS code<sup>6</sup> was used for the Monte Carlo calculations, where the geometry of the Ge detector was input and the measurement efficiency was calculated by scoring the energy imparted by electrons to the Ge crystal region for 22 monoenergetic  $\gamma$ -rays of 10 keV to 3 MeV.

### 3. Results and discussion

**3.1 Extraction of spherical particles.** For samples Uj01-01 to Uj01-02, a magnetic sample of about 0.5 g was obtained from sand samples of 150–250 g with a grain size of less than 1 mm, and about 0.15 g of spherical particles were extracted from each sample. The recovery rates of the samples are sum-

marized in Table 2. Spherical particles were recovered at a rate of about  $10^{-5}$  to  $10^{-3}$  for sand with a particle diameter of 1 mm or less around Moto-Ujina Beach. In the control samples taken from the similar sand beach around Takehara and Mihara regions, 1 or 2 spherical particles were observed at sampling locations CNT02 to CNT04. The particle size distribution for sample Uj05-02U (0.141 g) is shown in Fig. 4. The mean diameter was 249  $\mu\text{m}$  with one standard deviation of 70  $\mu\text{m}$ . Assuming a particle diameter of 249  $\mu\text{m}$  and a density of 2  $\text{g/cm}^3$ , the ratio of spherical particles to sand with a particle diameter of 1 mm or less was estimated to be about  $10^{-8}$  to  $10^{-7}$ , which is 1–3 orders of magnitude lower than that around Moto-Ujina Beach.

**3.2 SEM-EDS measurements.** The SEM images in Fig. 5 of the CL-L, CL-S, YL-M, YL-S, and BL-S particles show that they were nearly spherical and had crater-like depressions on their surfaces, similar to the radioactive particles found during the FDNPP accident investigation. The crater-like depressions are thought to be caused by the bursting of gas bubbles during agglomeration. In addition, the RD-S, BL-L, and BL-Tw particles had a slightly distorted spherical shape, which may be due to the adhesion of other substances to the

surface during the condensation processes.

Figure 6 shows the EDS spectra of the CL-S, YL-S, RD-S, and BL-L bulk, and the RD-S and BL-L surfaces. The elements C, O, F, Na, Mg, Al, Si, P, K, Ca, Ti, V, and Fe were identified. Most of the C signal was from the C tape on which the sample was placed. Therefore, it is intuitive to assume that these particles were formed by the vaporization and agglomeration of soil. The surface elemental analysis of the distorted RD-S and BL-L samples showed an increase in Fe on the surface, unlike the bulk samples.

There are several possible origins for such particles, including natural sources such as impact spherules, meteorite ablation spheres, and small-scale volcanic dust, as well as anthropogenic sources such as particulates from fireworks, steam locomotives, and the use of power tools such as gas fusion torches and angle cutters. Even the production or use of mineral fibers could be the source. However, all of these particles can have similar morphologies. Micrometeorite-derived particles are indicated in many cases by the presence of Ni-bearing iron metal or Mg-rich Ni containing Fe<sup>10</sup>. Genareau et al. reported that volcanic spherules contain Si with lower amounts of Al, K, Ca, and Fe<sup>11</sup>. There is a wide range of anthropogenic particulates having various origins, but

**TABLE 2: Sand samples with a grain size of 1 mm or less, magnet extraction volume, and particle extraction volume.**

Sample name	Sand mass (g)	Magnetically extracted sample (g)	Extracted particles (g)	Particles/sand
Uj01-01U	150.1	0.98	0.15	$9.99 \times 10^{-4}$
Uj01-01D	159.8	1.04	0.13	$8.14 \times 10^{-4}$
Uj01-02U	175.1	1.27	0.15	$8.57 \times 10^{-4}$
Uj01-02D	212.6	1.33	0.206	$9.69 \times 10^{-4}$
Uj02-01U	110.0	0.20	0.012	$1.09 \times 10^{-4}$
Uj02-01D	138.8	0.22	0.013	$9.37 \times 10^{-5}$
Uj02-02U	156.5	0.26	0.01	$6.39 \times 10^{-5}$
Uj02-02D	196.5	0.33	0.02	$1.02 \times 10^{-4}$
Uj03-01U	164.7	0.11	0.01	$6.07 \times 10^{-5}$
Uj03-01D	119.8	0.07	0.01	$8.35 \times 10^{-5}$
Uj03-02U	100.3	0.13	0.007	$6.98 \times 10^{-5}$
Uj03-02D	83.4	0.086	0.002	$2.40 \times 10^{-5}$
Uj04-01U	98.2	0.23	0.01	$1.01 \times 10^{-4}$
Uj04-01D	76.2	0.25	0.01	$1.31 \times 10^{-4}$
Uj04-02U	234.18	0.56	0.01	$4.26 \times 10^{-5}$
Uj04-02D	130.84	0.26	0.01	$7.64 \times 10^{-5}$
Uj05-01U	121.3	0.16	0.01	$8.24 \times 10^{-5}$
Uj05-01D	55.4	0.11	0.01	$1.81 \times 10^{-4}$
Uj05-02U	62.7	0.14	0.0196	$3.12 \times 10^{-4}$
Uj05-02D	77.6	0.20	0.0094	$1.21 \times 10^{-4}$
CNT01U	77.4	0.15	0	0
CNT01D	186	0.45	0	0
CNT02U	221	0.56	$1.62 \times 10^{-5}$ (1)*	$7.32 \times 10^{-8}$
CNT02D	231.5	0.71	$3.23 \times 10^{-5}$ (2)*	$1.40 \times 10^{-7}$
CNT03U	235.8	0.13	$1.62 \times 10^{-5}$ (1)*	$6.86 \times 10^{-8}$
CNT03D	273.5	0.13	$1.62 \times 10^{-5}$ (1)*	$5.91 \times 10^{-8}$
CNT04U	225.4	0.57	$3.23 \times 10^{-5}$ (2)*	$1.43 \times 10^{-7}$
CNT04D	280.8	0.62	$1.62 \times 10^{-5}$ (1)*	$5.76 \times 10^{-8}$
CNT05U	84.6	0.06	0	0
CNT05D	155.3	0.13	0	0

\*: Weight of one particle assuming a mean diameter of 249  $\mu\text{m}$  and a density of 2  $\text{g/cm}^3$ . The numbers in parentheses are the numbers of confirmed spherical particles.

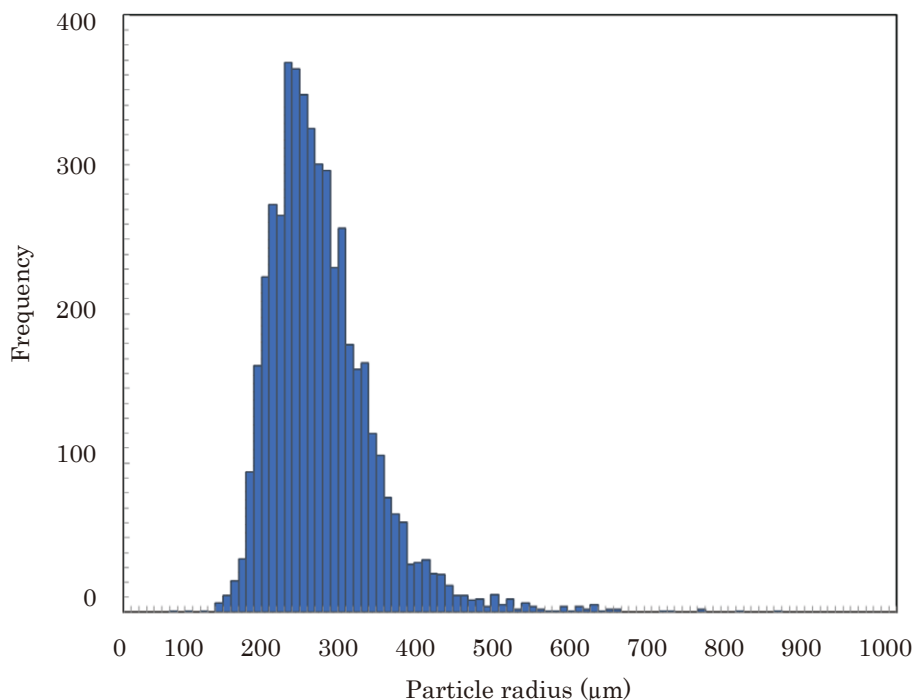


Figure 4. Particle size distribution for sample Uj05-02U.

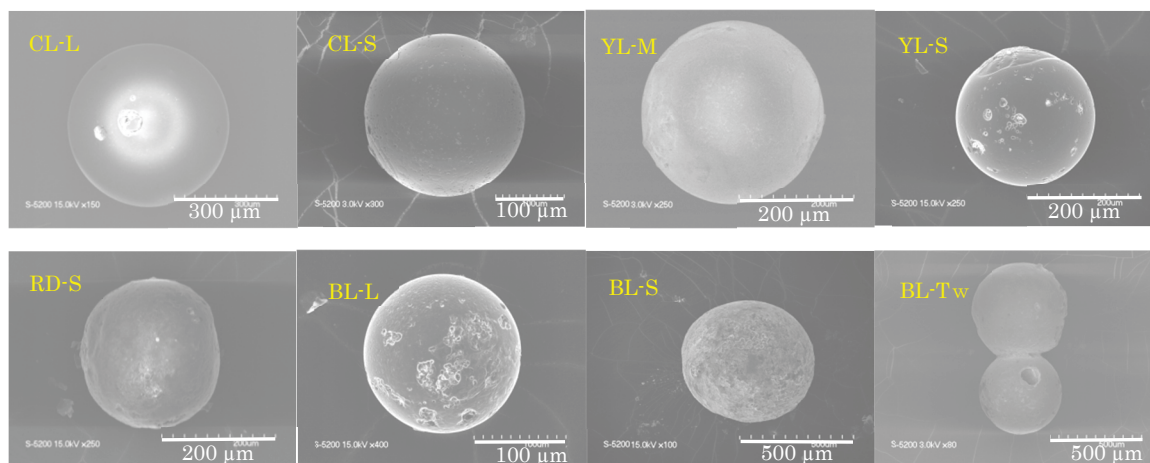


Figure 5. SEM images of CL-L, CL-S, YL-M, YL-S, RD-S, BL-L, BL-S, and BL-Tw particles.

iron oxide is often given off during the use of power tools, and particles from different colors of fireworks tend to contain metal salts of Sr/Li (red), Ca (orange), Na (yellow), Ba (green), and Al/Ti/Mg (silver/white)<sup>12</sup>.

The EDS spectra suggested that all CL-S, YL-S, RD-S, and BL-L particles contain Al, Ca, and Fe, and to a lesser extent Mg and Ni, suggesting a low possibility of a micrometeorite-derived origin. The other 12 elements were similar to the elemental components in the soil or the radioactive hot particles from the FDNPP accident<sup>5</sup>. Therefore, it is intuitive to assume that these particles were formed by the vaporization and agglomeration of soil or rocks. In the Chugoku region, Mt. Sanbe is estimated to have been volcanically active at least three times between 3600 and 4500 years ago<sup>13</sup>. The Abu volcano group is in neighboring Yamaguchi Prefecture, and the most recent eruption is estimated to be 8800 years ago<sup>14</sup>. The volcanic ejecta from these volcanic activities is mainly dacite but also includes fallen volcanic ash, pyroclastic flows, lava eruptions, formation of pyroclastic hills, and generation of volcanic mudflows. In particular, pyroclastic flows and volcanic mudflows can reach distant areas. If the spherical iron-rich

particles observed were of volcanic origin, we would expect to find the same amount of spherical iron-rich particles in the samples from the Takehara-Mihara area, which we used as a control. We found far fewer spherical particles in the control samples, suggesting that the spherical particles were not volcanic and could have originated from the atomic bomb explosion. Nevertheless, we could not exclude micrometeorites or domestic and industrial activities such as shipbuilding, automobile fabrication, and garbage incineration as sources for the spherical particles. It should also be noted that fireworks festivals have been held for many years on Miyajima, an island near Hiroshima that is one of the most popular tourist destinations in Japan.

**3.3 Ge measurement.** The results of Ge measurement of 5.86 g of spherical iron-rich particles and the background are shown in Fig. 7 as count rate spectra. The signals from the radionuclides were small and about twice as large as the background. In addition,  $^{210}\text{Pb}$ ,  $^{214}\text{Pb}$ ,  $^{214}\text{Bi}$ , and  $^{224}\text{Th}$  from the uranium series and  $^{208}\text{Tl}$ ,  $^{212}\text{Pb}$ ,  $^{212}\text{Bi}$ , and  $^{228}\text{Ac}$  from the thorium series were identified. Furthermore, although not statistically

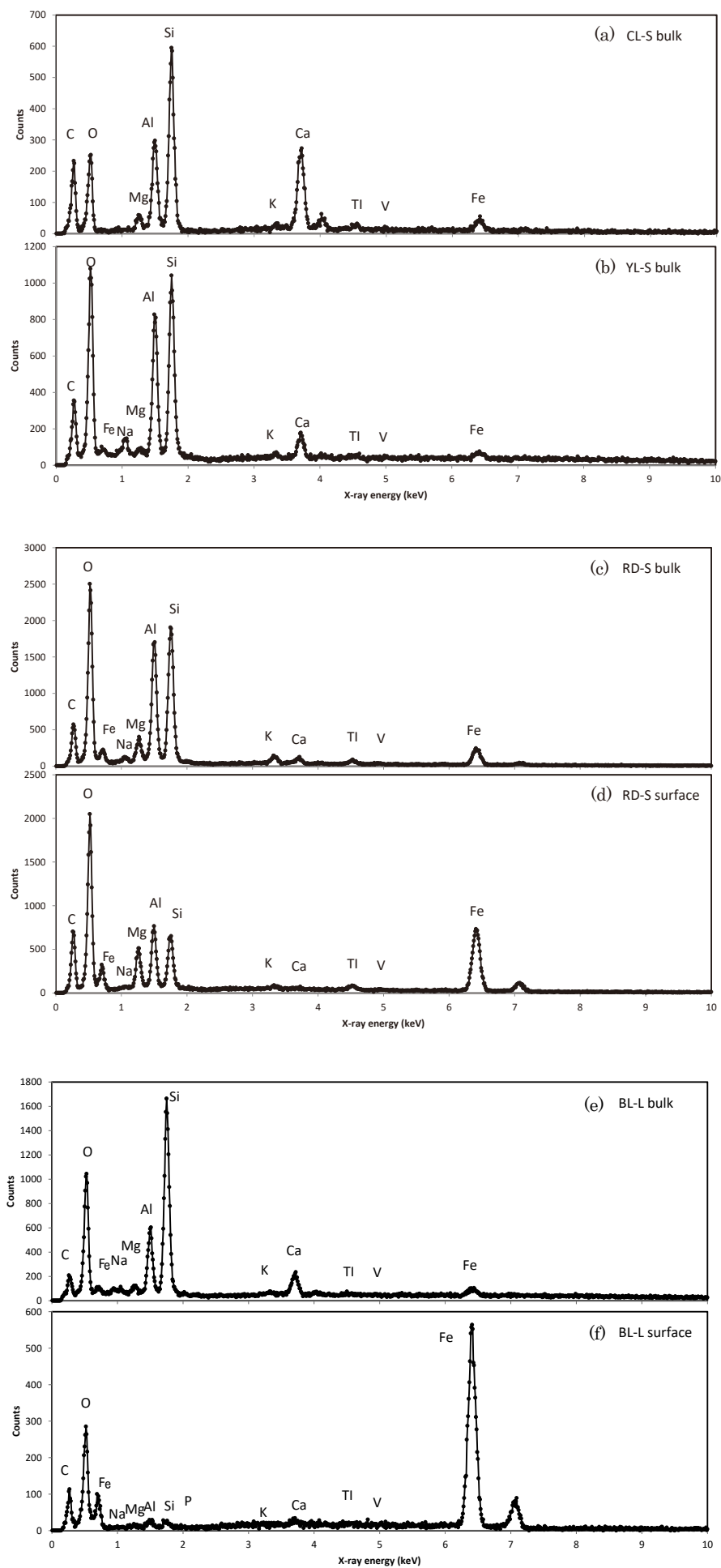


**Figure 6.** EDS spectra of the (a) CL-S bulk, (b) YL-S bulk, (c) RD-S bulk, (d) RD-S surface, (e) BL-L bulk, and (f) BL-L surface.

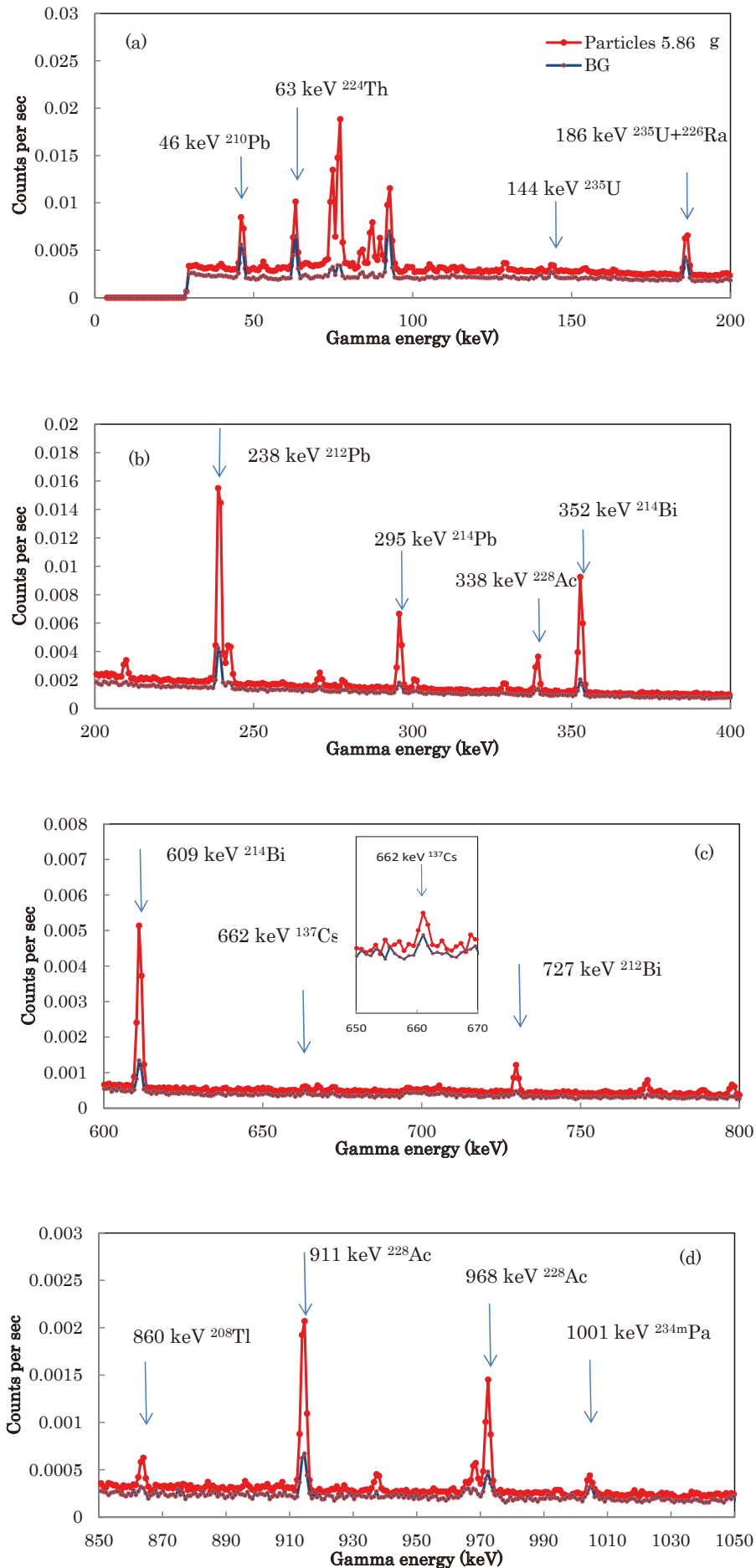


**Figure 7.**  $\gamma$ -ray spectra of the spherical particles measured with a Ge detector. (a) 0–200 keV region, (b) 200–400 keV region, (c) 600–800 keV region, and (d) 850–1050 keV region.

**TABLE 3: Radioactivity in the 5.86 g sample of spherical particles and sand.**

	Nuclide	Radioactivity in 5.86 g sample (mBq/g)	Radioactivity in sand (mBq/g)
U series	<sup>210</sup> Pb	86.9 ± 7.1	8.7 ± 6.8
	<sup>234</sup> Th	91.6 ± 7.9	7.7 ± 7.3
	<sup>226</sup> Ra	147.2 ± 11.4	23.2 ± 10.5
	<sup>214</sup> Pb	94.1 ± 1.7	9.7 ± 1.5
	<sup>214</sup> Bi	107.3 ± 6.0	8.2 ± 5.3
	<sup>234m</sup> Pa	119.8 ± 75.1	ND ± ND
Th series	<sup>212</sup> Pb	85.4 ± 1.3	8.2 ± 1.0
	<sup>228</sup> Ac	79.9 ± 4.4	13.0 ± 4.1
	<sup>208</sup> Tl	58.5 ± 5.4	4.7 ± 1.5
	<sup>235</sup> U	4.7 ± 2.5	ND ± ND
	<sup>137</sup> Cs	1.3 ± 0.5	0.5 ± 0.6
	<sup>40</sup> K	107.3 ± 6.0	8.2 ± 5.3

significant, the 1001 keV  $\gamma$ -rays from <sup>234m</sup>Pa and the 144 keV  $\gamma$ -rays from <sup>235</sup>U were slightly higher than the background. Also, a small amount of 662 keV <sup>137</sup>Cs  $\gamma$ -rays were detected. The radioactivity concentrations converted from these count rates are shown in Table 3. A sand sample of 5.86 g was also measured with the Ge detector. The signs in Table 3 show that the count rates for the 5.86 g spherical iron-rich particle sample were twice or more those of the 5.86 g sand sample; thus, the concentrations of the uranium and thorium series radionuclides in the spherical particle sample were different from those in the sand sample. The U, Th, and K concentrations in the particles were estimated to be 8.67 ppm, 20.06 ppm, and 0.35%, respectively. The U, Th, and K concentrations of the particles were slightly higher than those of the reference rock JG-3 for the Chugoku region<sup>15</sup> and those of the soil from Ohta River in Hiroshima City<sup>16</sup> (Table 4). This result suggests that the soil in Hiroshima may have provided the raw materials for the spherical iron-rich particles.

These results identified radon precursors in the uranium and thorium series, suggesting that <sup>234m</sup>Pa and <sup>235</sup>U may be present in very small amounts in the spherical iron-rich particles. However, no clear evidence of a U isotopic signature was observed. The ratio of <sup>235</sup>U/<sup>238</sup>U = 0.006727 ± 0.00503, which was calculated from <sup>235</sup>U and the averaged value of <sup>238</sup>U daughter concentrations, was similar to the natural abundance of 0.00726. To confirm the atomic bomb explosion origin of the spherical iron-rich particles, mass spectroscopy measurements, including inductively coupled plasma-mass spectroscopy (ICP-MS), should be performed.

#### 4. Conclusions

Sand samples were collected from the beach on Moto-Ujina Island in order to analyze spherical iron-rich particles, which may have been produced by the Hiroshima atomic bomb explosion. About 6 g of spherical particles were extracted from the sand samples collected from Moto-Ujina Beach. The extracted samples were analyzed by SEM-EDS and by  $\gamma$ -ray measurements with a Ge detector. SEM-EDS analysis revealed that the particles were composed mainly of Si and O and also contained Na, Mg, Al, Si, P, K, Ca, Ti, V, and Fe. The Ge detector measurements detected <sup>137</sup>Cs (1.3 ± 0.5 mBq g<sup>-1</sup>), radon progenies from the uranium series and thorium series, and small amounts of <sup>234m</sup>Pa and <sup>235</sup>U in spherical iron-rich particles. However, we still could not definitively conclude that the spherical iron-rich particles isolated from the Moto-Ujina

**TABLE 4: U, Th, and K concentrations in the spherical particles, reference rock JG-3 from the Chugoku region (Imai et al. 1995), and soil from the Ohta River in Hiroshima City (AIST 2022)**

	Particles	JG-3	Ohta River
U concentration	8.67 ppm	2.21 ppm	4.23 ppm
Th concentration	20.6 ppm	8.28 ppm	15.68 ppm
K concentration	0.35%	2.19%	2.04%

beach sand were generated by the Hiroshima atomic bomb explosion in August 1945, although origins from other sources do not appear to be realistic, as discussed by Wannier et al.<sup>3</sup> In future work, we will confirm the abundance of uranium isotopes in the particles from the Moto-Ujina beach by using mass spectroscopic measurements, such as ICP-MS and secondary ion mass spectrometry to draw a more definitive conclusion about the origins of the particles.

#### Acknowledgements

The SEM-EDS measurements were performed in the Natural Science Center for Basic Research and Development (N-BARD), Hiroshima University. The authors are grateful to the staff N-BARD. This study was carried out as a part of the “Study on the Construction of a Meteorological Simulation Model for the Atomic Bombings and the Analysis of Fallout Dispersion,” funded by the Ministry of Health, Labour and Welfare of Japan.

#### References

- [1] Hiroshima City, Revisit the Hiroshima A-bomb with a database, Edt. Aoyama M and Oochi Y, 978-4-9905935-0-6, 2011.
- [2] Hiroshima City, Revisit the Hiroshima A-bomb with a database Vol. 2, Edt. Aoyama M and Oochi Y, 978-4-9905935-1-3, 2013.
- [3] Wannier M.A. M, Urreiztieta M, Wenk H, Stan V. C, Tamura N, Yue B (2019) Fallout melt debris and aerodynamically-shaped glasses in beach sands of Hiroshima Bay, Japan, *Anthropocene* 25, 100196.
- [4] Adachi K, Kajino M, Zaizen Y, Igarashi Y (2013) Emission of spherical cesium-bearing particles from an early stage of the Fukushima nuclear accident. *Sci Rep* 2013; 3:2554.
- [5] Nakamura S, Kajimoto T, Tanaka T, Yoshida H, Maeda M, Endo S (2018) Measurement of <sup>90</sup>Sr radioactivity in cesium hot particles originating from the Fukushima Nuclear Power Plant Accident *J. Radiat. Res* 59 (6), 677–684.
- [6] Abe Y, Onozaki S, Nakai I, Adachi K, Igarashi Y, Oura Y, Ebihara M, Miyasaka T, Nakamura H, Sueki K, Tsuruta H, Moriguchi Y (2021) Widespread distribution of radio-cesium-bearing microparticles over the greater Kanto Region resulting from the Fukushima nuclear accident, *Prog Earth Planet Sci* 8, 13.
- [7] Onishi S, Thornton B, Koike T, Odano N, Asami M, Kamada S, Nagano K, Ura T, (2021) Analysis of radioactive cesium-enriched particles and measurement of their distribution in marine sediment near Fukushima Daiichi nuclear power plant, *J Nucl Sci Tech* 58 (4), 482-492.
- [8] Satou Y, Sueki K, Sasa K, Yoshikawa H, Nakama S, Minowa H, Abe Y, Nakai I, Ono T, Adachi K, Igarashi Y (2018) Analysis of two forms of radioactive particles emitted during the early stages of the Fukushima Dai-ichi Nuclear Power Station accident, *Geochem J* 52, 137-143.

- [9] The Geospatial Information Authority of Japan (GSI), Electronic map (GSI tile), <https://maps.gsi.go.jp/development/ichiran.html> 2021.8.24.
- [10] Genge M J, Engrand C, Gounelle M, Taylor S (2008) The classification of micrometeorites, *Meteoritics & Planet Sci* 43, Nr 3, 497–515.
- [11] Genareau K, Wardman J B, Wilson T M, McNutt S R, Izbekov P (2015) Lightning-induced volcanic spherules, *Geology* 43; 4, 319–322.
- [12] Noguchi K, Yoneda S, Takei M (2018) BIINSEKI TANSAKU ZUKAN, SOGENSHA Inc., ISBN 978-4-422-45003-2 C0044
- [13] Japan Active Volcanoes 4th Edition, Japan Meteorological Agency, 2013, [https://www.data.jma.go.jp/svd/vois/data/tokyo/STOCK/souran\\_eng/menu.htm](https://www.data.jma.go.jp/svd/vois/data/tokyo/STOCK/souran_eng/menu.htm) 2021.8.24.
- [14] Kudo T, Hoshizumi H, 2006-. Catalog of eruptive events within the last 10,000 years in Japan, database of Japanese active volcanoes. Geol Surv Japan, AIST, <http://riodb02.ibase.aist.go.jp/db099/eruption/index.html> 2021.8.24.
- [15] Imai, N., Terashima, S., Itoh, S. and Ando, A. (1995) 1994 Compilation of analytical data for minor and trace elements in seventeen GSJ geochemical reference samples, “igneous rock series”, *Geostandards Newsletter*, 19, 135-213
- [16] National Institute of Advanced Industrial Science and Technology (AIST), Elemental distribution in Japan: Geochemical map of Japan, <https://gbank.gsj.jp/geochemmap/>, 2022.2.14.